Effect on electron energy on amorphization of $ZrCr_2$

J. A. Faldowski and A. T. Motta
Department of Nuclear Engineering, The Pennsylvania State University, University Park, Pennsylvania 16802

L. M. Howe
AECL Chalk River Laboratories, Chalk River, Ontario K0J 1J0, Canada

P. R. Okamoto
Materials Science Division, Argonne National Laboratory, 9700 South Cass Avenue, Argonne, Illinois 60439

(Received 6 November 1995; accepted for publication 5 April 1996)

The influence of electron energy on the amorphization of $ZrCr_2$ at 25 K was measured. Amorphization was observed at electron energies from 900 to 330 keV. The dose-to-amorphization increases with decreasing electron energy with two steps, one at 700 keV corresponding to the decrease in the Zr displacement cross section due to the approaching displacement threshold of Zr and one at 500 keV corresponding to an appreciable decrease in the displacement cross section of Cr due to the approaching displacement threshold for Cr. At lower electron energies, it is believed that amorphization occurs principally through a secondary displacement mechanism, where light impurity atoms (mainly O) are displaced by electrons and displace in turn the heavier atoms. By fitting the results using electron displacement cross sections, we find the displacement energies in each sublattice to be $E_d^{Zr} = 22$ eV, $E_d^{Cr} = 23$ eV, $E_d^{O} = 4$ eV. © *1996 American Institute of Physics.* [S0021-8979(96)02914-3]

I. INTRODUCTION

Since amorphization of intermetallic compounds was shown to occur under electron irradiation[1,2] there has been great interest in trying to elucidate the mechanisms of the transformation. This is because displacement cascades are absent under electron irradiation and amorphization mechanisms prevalent in ion and neutron irradiation (such as direct amorphization upon cascade cooling[3] or amorphization by cascade superposition[4]) do not occur. Consequently, amorphization has to result from the slow buildup of accumulated point defects and chemical disorder and is, therefore, directly related to the mobility and characteristics of the individual defects.

In a binary intermetallic compound, there are at least six types of point defects: interstitials of either type of atom, vacancies in either sublattice and antisite defects in either sublattice. Those defects have different migration and formation energies and different interaction energies with sinks and other point defects. Recognizing this, the annealing stages observed in the dose-to-amorphization versus temperature curve of various intermetallic compounds have been attributed to the thermal activation of different defects at various temperatures.[5] However, what is not often considered is that the rate of defect creation in the individual sublattices is different (due to the different masses of the atoms and to the different bonding in each crystallographic site). This causes the displacement energy for the two atoms in the compound to be different, in principle, as demonstrated in Zr_3Fe,[5,6] $ZrCr_2$,[7] and Zr_2Fe.[7]

The object of this article is to further investigate this hypothesis in the compound $ZrCr_2$ by using the dose-to-amorphization at low temperature to measure the displacement energies in the Cr and Zr sublattices. Particular emphasis is placed on developing a method of analysis (including a detailed estimation of errors involved) that is generally applicable in determining the displacement energies of the constituent atoms in intermetallic compounds.

II. EXPERIMENTAL METHODS

The samples used in this study were prepared at Chalk River Laboratories. Arc melting of elemental Zr (99.8%) and Cr (99.99%) with an overall atomic ratio of 1.22 (55% Zr and 45% Cr), produced a button of the alloy. The alloy was heat-treated for 2 h at 1173 K followed by 48 h at 1073 K. Thin disks, 3 mm diam and 0.1 mm thick, were prepared by cutting a slice from the annealed button, grinding it down mechanically and cutting with a spark-cutter. The disks were then electropolished in a twin jet electropolisher using a solution of 10% perchloric acid and methanol, kept at 223 K. Preirradiation examination conducted in a Philips CM-30 at Chalk River Laboratories, found the resulting microstructure to be a mixture of α-Zr and a Zr–Cr phase. Electron diffraction patterns obtained for the Zr–Cr phase were consistent with a $MgCu_2$-type C15a $ZrCr_2$ phase.[8] Chemical analysis by energy dispersive x-ray (EDX) confirmed the approximate composition of $ZrCr_2$.

The irradiations were conducted in the Kratos HVEM in the Center for Electron Microscopy at Argonne National Laboratory. At 25 K, the experiments consisted of selecting an area with a low index bend contour, condensing the beam, and recording the progress of the transformation by taking both bright field or dark field pictures and diffraction patterns at regular intervals. The sample was judged to be amorphous when the bend contour contrast exhibited a milky appearance and the spots in the diffraction pattern were replaced by diffuse rings. The size of the smallest diffraction aperture was

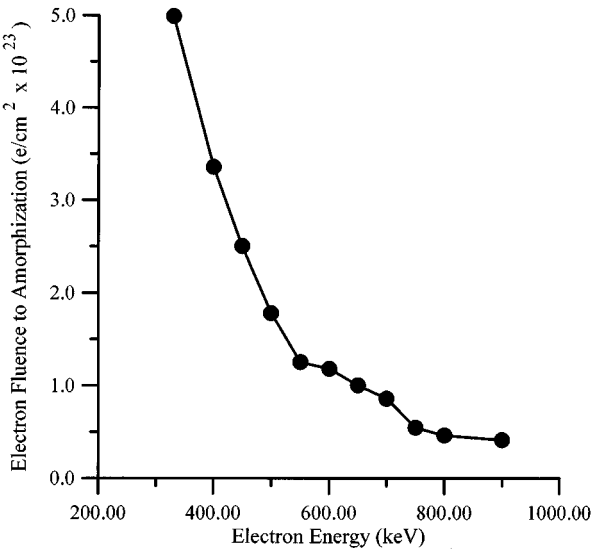

FIG. 1. Measured dose-to-amorphization of $ZrCr_2$ as a function of electron energy.

about 0.3 μm, so the electron doses reported are the doses necessary to attain an amorphous spot of that size.

The voltage was varied between 900 and 330 keV. We attempted to maintain the same current density at the center of the beam throughout the experiment, but the changing microscope conditions with voltage made that impossible. The electron current and, therefore the displacement rate, decreased by 32% as the electron energy went from 900 to 330 keV. It was previously determined for Zr_3Fe (Ref. 9) that at 25 K such a change in the displacement rate does not have major impact on the dose to amorphization. This is also expected to be the situation for $ZrCr_2$.[10] The shape of the electron beam was determined by measuring the peak current density and the overall current using two separate Faraday cages. Beam heating was estimated to be of the order of a couple of degrees K. The vacuum was $1-2\times10^{-7}$ Torr. Post irradiation examination was conducted in a Philips 420 TEM at the Materials Characterization Laboratory at Pennsylvania State University and in a JEOL 100 CX at Argonne National Laboratory.

III. RESULTS

The dose-to-amorphization versus electron energy in $ZrCr_2$ is shown in Fig. 1. As the electron energy decreases from 900 to 750 keV, there is not much change in the dose-to-amorphization. As the electron energy decreases from 750 to 650 keV, there is a step increase in the dose-to-amorphization which then remains constant until an electron energy of about 550 keV. Below 550 K the dose-to-amorphization increases abruptly. Amorphization becomes increasingly difficult to achieve below 440 keV during practical irradiation times. Similar steps in the variation of the dose to amorphization with electron energy were observed in other compounds.[6,7]

In all the irradiations conducted, amorphization followed a similar pattern, exhibiting ''transformation stages'' that, although subjective, proved to be quantifiable. By analyzing numerous experiments, it became clear that the point in the irradiation at which an amorphous ring was first considered to be visible in the microscope was very reproducible, and occurred at 15% of the total irradiation time. At about 85% of the irradiation time, the outer spots on the diffraction pattern have disappeared and only those with a spacing close to that of the ring remain. We used this fact to complete our data set because two of our lowest energy experiments were not taken to completion due to the fact that diffraction spots not visible in the microscope at the end of the irradiation were visible on the film. In both cases, however, they had been taken to the 85% stage and we extrapolated those values to obtain the final dose. We checked this by running the same extrapolation from the 15% dose, and obtained the same result for the extrapolation to 100% dose, within a 5% error.

IV. ANALYSIS

The experimental results are analyzed assuming that amorphization occurs at a critical electron dose. This critical dose is dependent on temperature and is specific to the compound, but is independent of electron energy. The apparent variation of the dose-to-amorphization with electron energy shown in Fig. 1 is just an indication of the variation of the damage production rate with electron energy. The dose to amorphization $D(E)$ at energy E, is given by

$$D(E)=\left[\Phi_e\sum_i x_i\sigma_d^i(E,E_d^i)\nu_i(E)\right]t(E), \tag{1}$$

where Φ_e is the electron flux, $t(E)$ is the measured time to amorphization under an electron flux of energy E, x_i is the concentration of element i in the compound, E_d^i is the displacement energy of atom i in the compound, $\nu_i(E)$ is the average number of secondary displacements caused by the recoils of atom i when produced by electrons of energy E, and σ_d^i is the displacement cross section of element i in the compound. In the present study, we fixed $\nu_i(E)=1$, which is justified since the primary and cascade cross sections in this case are nearly equal.[11]

According to the model above, for all electron energies amorphization occurs at a constant level of displacements per atom $D_{\rm crit}$, so the amorphization condition is

$$D(E)=D_{\rm crit} \tag{2}$$

Two main points should be noticed from the data. (1) Amorphization occurs even at very low electron energies. This suggests that a secondary displacement mechanism[12,13] might be in operation, where light impurity atoms (O in particular) are displaced by electrons and these light impurity atoms then displace the heavier constituent atoms in the intermetallic compound. (2) There are two breaks in the curve indicating two shifts in regime.

By fitting the curve in Fig. 1 to make Eq. (1) valid, we can determine the various E_d^i corresponding to the displacement energies of the individual atoms in the compound. This can be done because for a given electron energy, the σ_d^i are only a function of E_d^i.[11] By systematically varying the E_d^i, it is possible to optimize the fit, and to determine the E_d's.

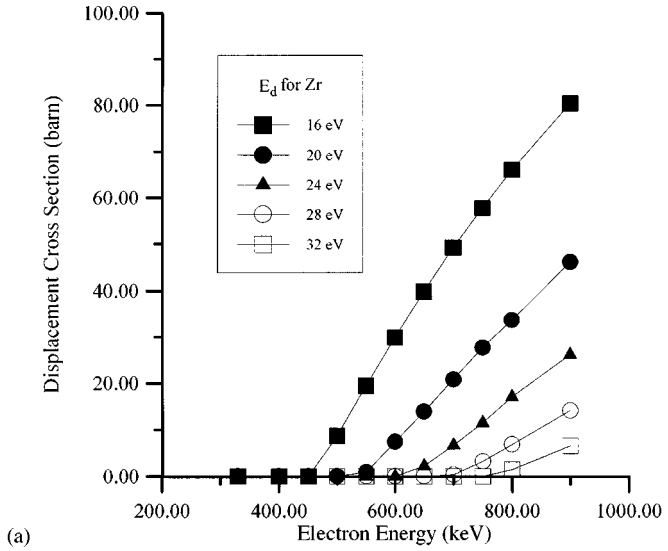

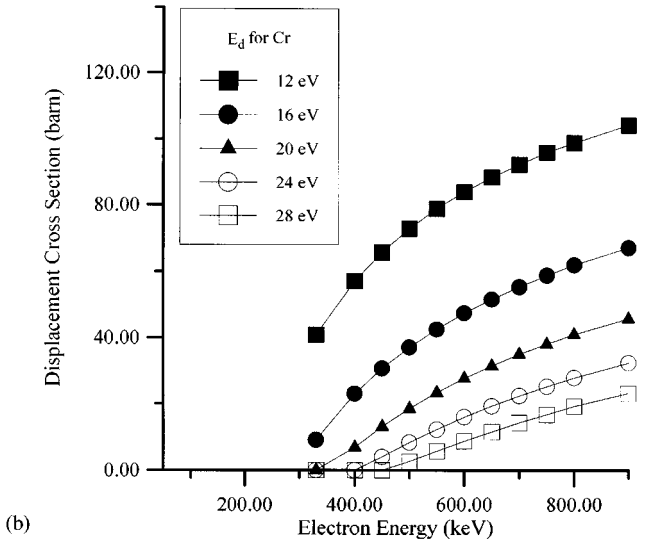

FIG. 2. (a) Zr displacement cross section vs electron energy for various displacement energies. (b) Displacement cross section vs electron energy for Cr for various displacement energies (see Ref. 11).

There are three fitting parameters, so a systematic search must be made for the best fit. We define the error of the fit as

$$\epsilon(E_d^{\mathrm{Cr}},E_d^{\mathrm{Zr}},E_d^{\mathrm{O}})=\sum_{j=1}^{N}\left[\frac{D(E_j)-\overline{D}}{\overline{D}}\right]^2, \tag{3}$$

where E_d^{Cr}, E_d^{Zr}, E_d^{O}, are the displacement energies for Cr, Zr, and impurity oxygen atoms in the compound $ZrCr_2$ and $D(E_j)$ is the dose to amorphization (in dpa) at electron energy E_j, calculated from Eq. (1) using the cross sections obtained from Ref. 11 by fixing the E_d's to specific values. $\overline{D}$ is the mean dose given by

$$\overline{D}=\sum_{i=1}^{N}\frac{D(E_i)}{N}. \tag{4}$$

The fitting procedure uses the displacement cross sections for electron irradiation as a function of electron energy, which were calculated by Oen[11] for various displacement energies. The curves for Zr and Cr are shown in Fig. 2. The

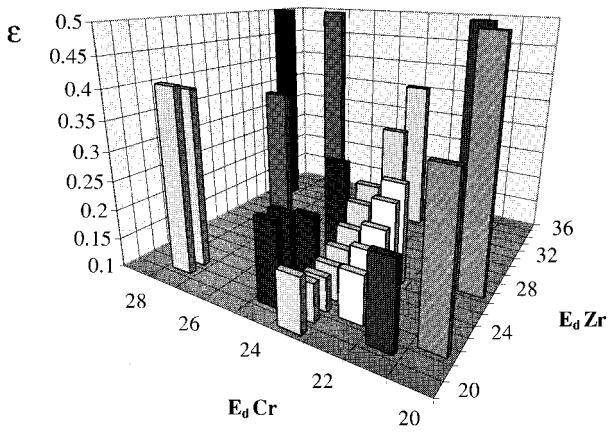

FIG. 3. Error of the fit [Eq. (3)] as a function of the displacement energies for both types of atoms.

fitting procedure was as follows

(1) Choose a set $(E_d^{\mathrm{Zr}},E_d^{\mathrm{Cr}},E_d^{\mathrm{O}})$. This determines the displacement cross sections σ_d^i as a function of electron energy.
(2) For each measured electron energy, calculate $D(E)$ by multiplying σ_d^i by $\Phi_e(E)t(E)$.
(3) Calculate D from Eq. (4).
(4) Calculate ϵ from Eq. (3).
(5) Repeat until a minimum value of ϵ is obtained.

The change in the error ϵ as E_d^{Cr} and E_d^{Zr} vary from 20 to 30 eV is shown in Fig. 3. It can be seen that there is a definite and unique minimum. The values that minimize the error are $E_d^{\mathrm{Cr}}=23$ eV, $E_d^{\mathrm{Zr}}=22$ eV, and $E_d^{\mathrm{O}}=4$ eV. The mean dose at amorphization is 1.85 dpa, considerably higher than that of either Zr_3Fe or Zr_2Fe.[6,7]

In Fig. 1, the break in the curve at 700 keV corresponds to the E_d of the heavier atom, in this case Zr. Above 700 kV, both atoms can be displaced directly. Below 700 keV, the Zr displacement cross section falls quickly with energy, so that the majority of displacements are initiated in the Cr sublattice. Below 500 keV, the Cr displacement cross section starts to decrease, until at 400 and 330 keV, the majority of the displacements are secondary displacements caused by electrons displacing light-atom impurities. The light-atom impurity can then strike Cr or Zr atoms in the compound and because of its much larger energy transfer parameter compared to electrons, transfer enough energy to either atom to cause secondary displacements in either sublattice. An oxygen concentration of 2 at. % was determined for the $ZrCr_2$ alloy using a forward elastic recoil detection technique.[7]

It can be seen from the above analysis that displacements are possible throughout the electron energy range, but become more improbable as the energy decreases. Above 700 keV, any struck atom can be displaced directly. Between 700 and 500 keV, σ_d^{Zr} decreases to zero so that only 2/3 of the atoms can contribute effectively to the total displacement rate. Below 500 keV, only 1% of the atoms have a significant displacement cross section. The curve of the total displacement cross section versus electron energy is shown in Fig. 4. Multiplying Fig. 1 by Fig. 4 for the optimized set of E_d's

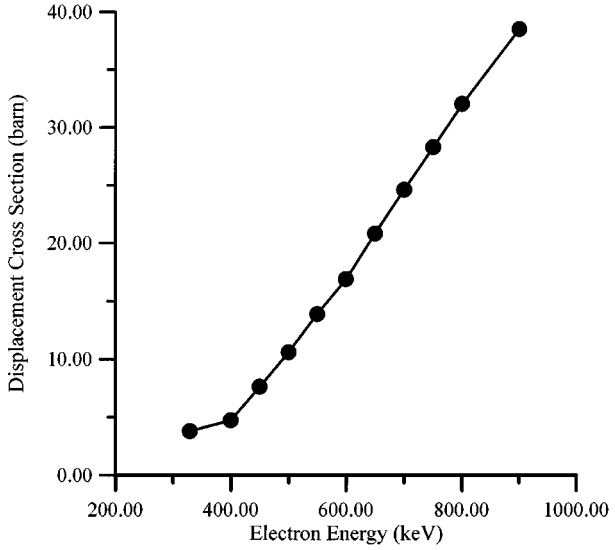

FIG. 4. Total displacement cross section for the optimized displacement energies.

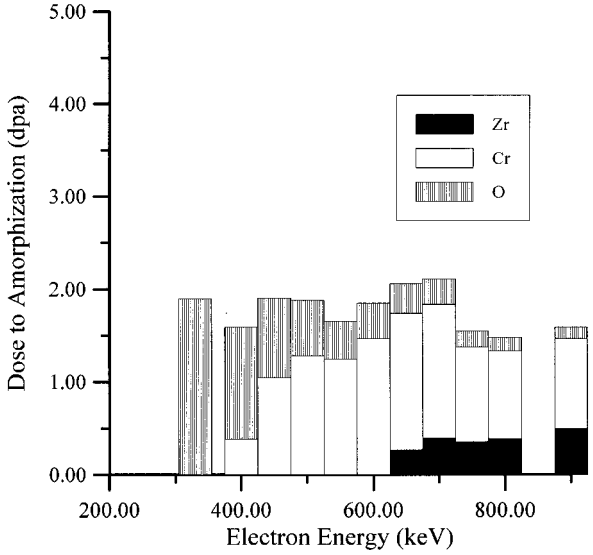

FIG. 6. Breakdown of individual contributions of the component atoms in initiating displacement damage, as a function of electron energy.

gives the curve in Fig. 5. Very good agreement is obtained, the calculated dose-to-amorphization in dpa not varying by more than 15%.

The breakdown of the relative contributions of each type of atom to the overall displacement rate is shown in Fig. 6. For the higher energies, both Cr and Zr displacements are dominant. In the intermediate region, the Cr contribution becomes the most important, and at lower energies the contribution of secondary displacements plays a key role. It should be emphasized that the stages in the dose-to-amorphization do not correspond directly to the threshold energies of the different atoms, but rather to points in the curve where the displacement cross sections taper off.

It is also worthy of note that the stages of the *in situ* amorphization process were very reproducible, always occurring at fixed percentages of the total amorphization time. This suggests that the amorphization mechanism was the same, regardless of the electron energy, and regardless of which atoms contribute more to the overall displacement rate.

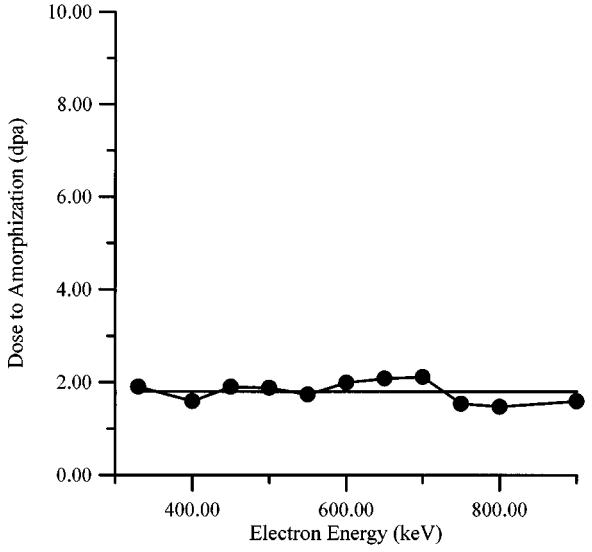

FIG. 5. Dose-to-amorphization vs electron energy for the optimized displacement energies.

V. DISCUSSION

The method employed here is similar to that used to find the displacement energy in pure metals, i.e., finding the electron energy below which the production of visible damage in the form of point defects or dislocation loops ceases. Frequently extended defects are not formed in intermetallic compounds under irradiation. The general irradiation response of intermetallic compounds is to undergo amorphization, so this is what we used to measure the displacement energies in the two sublattices. Compared to similar analyses done in Zr_3Fe[5,6] and Zr_2Fe,[7] the dose-to-amorphization of $ZrCr_2$ is much higher (by factors of 7 and 45). This is consistent with the fact the dose-to-amorphization of $ZrCr_2$ under ion irradiation is higher than that of Zr_3Fe.[14] It is also consistent with the fact that Zr_2Fe can be made amorphous by electron irradiation over a wider temperature range of temperature than $ZrCr_2$.[10] It would be interesting to perform this experiment for the compound $ZrFe_2$, which although it has the same crystalline structure as $ZrCr_2$, has a much lower critical temperature (100 K vs 200 K).[10]

A similar analysis of the data from experiments on the electron energy dependence of amorphization of Zr_2Fe and Zr_3Fe yielded the following values of the threshold displacement energies:

(1) orthorhombic Zr_3Fe: $E_d^{Cr} = 26$ eV, $E_d^{Zr} = 18$ eV, and $E_d^{O} = 12$ eV.
(2) tetragonal Zr_2Fe: $E_d^{Zr} = 25$ eV, $E_d^{Cr} = 27$, and $E_d^{O} = 8$ eV.
(3) cubic Laves phase $ZrCr_2$: $E_d^{Cr} = 23$ eV, $E_d^{Zr} = 22$ eV, and $E_d^{O} = 4$ eV.

The results show that the differences between the E_d^i values on the sublattices (Zr, Fe or Cr) of the above intermetallics are greatest for Zr_3Fe and least for $ZrCr_2$.

Having determined the specific E_d^i for the constituent atoms on the sublattices of Zr_2Fe, Zr_3Fe, and $ZrCr_2$, it is now possible to accurately compute doses (in dpa) during irradiation of these compounds with electrons, neutrons, or ions, i.e., it is no longer necessary to assume an effective E_d value for the compound. The present results also show the importance of secondary displacement events produced by light element impurities in these compounds. This is an important effect to be aware of since most zirconium alloys are likely to contain relatively large concentrations of O and N.

The displacement energy for oxygen in the compound, E_d^{O}, was quite low (4–12 eV) for Zr_3Fe, Zr_2Fe, and $ZrCr_2$. Elements such as H, N, and O, which have small atomic radii (0.078, 0.088, and 0.089 nm, respectively) relative to Zr (0.16 nm), are expected to occupy interstitial positions in the hcp lattice of α-Zr.[15] Most likely, these same elements will occupy interstitial positions in the lattice of Zr_3Fe, Zr_2Fe, and $ZrCr_2$. Consequently, the low values of E_d^{O} for these compounds probably reflect the relative ease of displacing interstitial O atoms in these structures.

VI. CONCLUSIONS

The influence of electron energy on the amorphization of $ZrCr_2$ at 25 K was measured at electron energies from 900 to 330 keV. The dose-to-amorphization increased with decreasing electron energy, with two steps, one at 700 keV corresponding to the decrease in the Zr displacement cross section due to the approaching displacement threshold of Zr and one at 500 keV corresponding to an appreciable decrease in the displacement cross section of Cr as its displacement threshold is approached. At lower electron energies, it is believed that amorphization occurs principally through a secondary displacement mechanism, where light element impurities (mainly O) are displaced by electrons and they in turn displace the heavier atoms (Zr and Cr). From a detailed analysis of the data, the displacement energies in each sublattice of $ZrCr_2$ were found to be $E_d^{\mathrm{Cr}} = 23$ eV, $E_d^{\mathrm{Zr}} = 22$ eV, and $E_d^{\mathrm{O}} = 4$ eV. The experimental technique and method of analysis used here should prove to be a general method for deriving displacement energies in intermetallic compounds that go amorphous under irradiation.

ACKNOWLEDGMENTS

The authors would like to thank D. Phillips of Chalk River Laboratories and B. Kestel of Argonne National Laboratory (ANL) for their expert help in sample preparation. Our thanks also go to Ed Ryan and Stan Ockers of Argonne for their excellent technical assistance with the HVEM. Joseph Faldowski was supported by a lab-grad fellowship from the Division of Educational Programs at ANL. This work was partly funded through a CANDU Owners Group (COG) contract. We wish to thank the COG Working Party-32 committee for their financial support and interest in the program.

[1] A. Mogro Campero, E. L. Hall, J. L. Walter, and A. J. Ratkowski, *Metastable Materials Formation by Ion Implantation*, edited by S. T. Picraux and W. J. Choike (Elsevier, New York, 1982), p. 203.
[2] G. Thomas, H. Mori, H. Fujita, and R. Sinclair, Scr. Metall. **16**, 589 (1986).
[3] L. M. Howe and M. Rainville, Philos. Mag. A **39**, 195 (1979).
[4] E. P. Simonen, Nucl. Instrum. Methods Phys. Res. B **16**, 198 (1986).
[5] A. T. Motta, L. M. Howe, and P. R. Okamoto, Mater. Res. Soc. Symp. Proc. **373**, 183 (1995).
[6] A. T. Motta, L. M. Howe, and P. R. Okamoto, Mater. Res. Soc. Symp. Proc. **316**, 265 (1993).
[7] L. M. Howe, D. Phillips, H. Zou, J. Forster, J. A. Davies, A. T. Motta, J. A. Faldowski, and P. R. Okamoto, Nucl. Instrum. Methods Phys. Res. B (in press).
[8] D. Arias and J. P. Abriata, Bull. Alloy Phase Diag. **7**, 237 (1986).
[9] A. T. Motta, L. M. Howe, and P. R. Okamoto, J. Nucl. Mater. **205**, 258 (1993).
[10] A. T. Motta, J. A. Faldowski, L. M. Howe, and P. R. Okamoto, Proceedings of the 11th ASTM International Symposium on Zirconium in the Nuclear Industry, Garmisch-Partenkirchen, Germany, September 1995 (in press).
[11] O. S. Oen, ORNL Report No. 4897 1973.
[12] P. G. Regnier, N. Q. Lam, and K. H. Westmacott, J. Nucl. Matter **115**, 286 (1983).
[13] P. Lucasson, J. Microsc. **16**, 183 (1973).
[14] L. M. Howe and D. Phillips (unpublished).
[15] L. M. Howe and M. L. Swanson, Nucl. Instrum. Methods Phys. Res., B **64**, 246 (1992).